Fermi National Accelerator Laboratory

TM-699
0310.000

CHARGE CHANGING METHODS FOR H^- INJECTION INTO THE BOOSTER SYNCHROTRON

Marshall Joy

Fermi National Accelerator Laboratory*
November 22, 1976

INTRODUCTION

A pulsed ORBUMP magnet transfers the incident 30 mA, 200 MeV H^- beam and the circulating proton beam into the same phase space. The combined $H^- - p^+$ beam passes through a stripping foil to convert $H^- \rightarrow H^+ e^- e^-$, resulting in a higher density proton beam which is then bent back to the design orbit. Several stripping foils, laser systems, and other arrangements will be examined.

I. THIN FOILS

Poly-para-xylylene foils were developed at Argonne National Laboratory for H^- injection into the ZGS booster. These foils are 90% carbon, 10% hydrogen by weight. The foil thickness used is 2500-5000 $\mathring{A}$, corresponding to the ANL linac beam energy of 50 MeV. At the Fermilab energy of 200 MeV the foils should be about four times thicker due to the approximate proportionality $dE/dx \sim E^{-1}$.

Operated by Universities Research Association Inc. under contract with the Energy Research and Development Administration

Argonne's efforts have been toward thinner foils to reduce multiple scattering. However, 2500 Å foils are very fragile indeed, and they become nearly impossible to work with when made much thinner than this. Also, the stripping efficiency is exponentially related to the foil thickness, and improvement of the RMS scattering entails a decrease in conversion efficiency. The reaction $H^- \rightarrow H^+ e^- e^-$ has an efficiency given by:

$$N_+ = 1 - \frac{\sigma_{-10} e^{-\sigma_{01} x} - (\sigma_{01} - \sigma_{-11}) e^{-(\sigma_{-10} + \sigma_{-11}) x}}{\sigma_{-10} + \sigma_{-11} - \sigma_{01}} \qquad (1)$$

where N_+ is the relative number of positive ions,
σ_{if} is the differential cross-section for the reaction

$$H^i \rightarrow H^f + (f-i)\, e^-,$$

and x is the parameterized penetration length in atoms/cm^2.

The associated RMS multiple scattering angle is

$$\langle\theta^2\rangle = \frac{.015}{\beta p} \left(\frac{L\eta}{L_{RAD}}\right)^{\frac{1}{2}}$$

$\beta = v/c = \left(\frac{\gamma^2 - 1}{\gamma^2}\right)^{\frac{1}{2}}$

$p = mv\gamma = (GeV/c)$

n = number of turns through foil

L = foil thickness (gm/cm^2)

L_{RAD} = radiation length of substance (gm/cm^2)

A combination of these two equations yields Fig. 1, conversion efficiency vs. θ_{RMS} per turn in various foils. Fig. 2 displays foil thickness vs. conversion efficiency. The required cross-sections are obtained from G. Marmer's[1] graph of σ vs. E for different substances (Fig. 3) which has been transferred into σ vs. Z at 200 MeV (Fig. 4). Marmer's data have already been extrapolated from 15 MeV, and further extension to 200 MeV is warranted only by the theoretical and low-energy experimental decline of $\sigma \sim E^{-1}$.

Parylene foils are fairly easy to make, but have low durability and relatively short lifetimes. Foils tested at ANL have lifetimes of about 5×10^{18} H^- with large statistical fluctuations. Preliminary results at Fermilab support this number, which corresponds to a few hours of running time. The only workable loading mechanism has been an oversized slide-projector with the foils mounted on 10cm x 6cm C-shaped holders. Parylene foils become exceedingly fragile after being irradiated, rupturing or dissociating when vacuum is released or upon removal. Although parylene foils do not melt, the polymers tend to curl up producing serious deformation at higher beam intensities. Plastic food wrap similar in thickness and composition to parylene was irradiated in the Fermilab booster with a disastrous loss of all beam in 100 μsec, probably due to impurities and granularity. Parylene foils are formed by sublimating poly-para-xylylene powder onto glass plates and can be made quite uniform and pure.

METALLIC FOILS

Metals can provide greater foil strength and increased lifetime but with an experimentally undetermined amount of scattering. Cross-sections in metals are found or extrapolated from Fig. 4.

For a particular stripping efficiency, the lowest possible atomic number is preferred. The fixed efficiency implies that the multiple scattering will be approximately constant, while the low Z enables the foils to be thicker and more resilient. Lithium and Beryllium are obvious choices.

Lithium's density of .53 g/cm^3 results in a desired thickness of 5 to 10 μm, corresponding to Parylene thickness of 1 to 2 μm. Though 5 → 10μm Lithium is available, it is not a very strong metal and melts at a relatively low temperature of 179°C. It also reacts strongly with water, and requires handling in vacuo or in an atmosphere of < 5ppm H_2O.

Beryllium is a much stronger and more stable metal, which melts at 1278°C. Be density of 1.85 yields a foil from .5 to 2μm, thicknesses close to those of parylene. Very thin Beryllium has only recently become available and has not yet been rolled

in the 2 μm range. Electroplating is an untested possibility. If thin Beryllium retains its tensile strength it should make an ideal stripping material with long lifetime.

Higher Z metals, i.e. Aluminum, Titanium, Vanadium, Chromium, Steel, and alloys of these, do not appear to be useful because of the required thicknesses in the .05 → .5 μm range. The scattering angle is increased slightly for these metals. (See Fig's 1,2)

The radiative equilibrium temperature can be calculated using Stefan's law: $P = \sigma\varepsilon T^4$. Equilibrium is reached when the energy delivered by the beam equals the radiative losses: radiative power

$$\text{flux} = \sigma\varepsilon\,(T_E^{\,4} - T_I^{\,4}) = \frac{\text{beam energy delivered}}{\text{cm}^2\text{sec}}$$

T_E = equilibrium temperature

T_I = initial (room) temperature

σ = stefan-boltzmann constant = $5.67 * 10^{-5}$ $\dfrac{\text{erg}}{\text{cm}^2\text{sec}\ {}^\circ\text{K}^4}$

ε = emissivity

$$\text{power flux} = \left(\frac{\text{energy loss}}{\text{proton}}\right)\left(\frac{\text{protons}}{\text{sec}}\right)\left(\frac{1}{\text{area}}\right)$$

$$= \left[\frac{dE}{dx}\left(\frac{\text{MeV}}{\text{gm/cm}^2}\right) * L(\text{gm/cm}^2)\right]\left[N\left(\frac{\text{protons}}{\text{turn}}\right) * \frac{\eta^2}{2}\left(\frac{\text{turns thru foil}}{\text{injection}}\right) * \nu\left(\frac{\text{injec}}{\text{sec}}\right)\right] * \left(\frac{1}{\text{Area}}\right)$$

$$= \frac{dE}{dx}\, L\, N\, \frac{\eta^2}{2}\, \frac{\nu}{A} * \left(1.6 * 10^{-6}\ \frac{\text{erg}}{\text{MeV}}\right)$$

$$\Rightarrow \quad T_E^4 = 1.6\times10^{-6} \quad \frac{\frac{dE}{dx} \; L \; N \; \frac{\eta^2}{Z} \; \frac{\nu}{A}}{\sigma \; \varepsilon} + T_I^4$$

From Fig. 5 we can extrapolate dE/dx at 200 MeV for Lithium. Assume 95% conversion efficiency => L = 320 $\mu g/cm^2$, linac current = 30 mA => N = $5*10^{11}$, number of turns (η) = 25 and further assume that the beam uniformly irradiates a 4 cm^2 section of the foil.
ε = .2, ν = 15 Hz, A = 4 cm^2, T_I = 300°K.

$$\Rightarrow T_E^4 = \frac{3.41 * 320\times10^{-6} * 5\times10^{11} * \frac{25^2}{2} * \frac{15}{4} * 1.6\times10^{-6}}{5.67*10^{-5} * .2} + (300)^4$$

$$T_E^4 = 9.83 * 10^{10} \; {}^{\circ}K^4$$

$$\Rightarrow T_E = 560^{\circ}K \text{ or } 285^{\circ}C.$$

The melting point of lithium is 180°C. The calculation is in two respects somewhat pessimistic. First, the area of the foil which is hit by the beam can be considered to be defined by the present Booster acceptance. This gives an area of 8.5 cm^2. Further, the cooling radiation emanates from both sides of the foil, giving another factor of 2 in area. An effective area of 17 cm reduces T_E to 141°C. Second, the average duty factor is usually lower than 15 Hz. Assuming further a main ring cycle period of 5 seconds further reduces T_E to 129°C. The pessimistic calculation for Beryllium (ε = .35) yields T_E = 460°K or 190°C which is well below the 1278° melting point.

II LASER INDUCED PHOTOIONIZATION

In the ≈ 1 meter long cavity between the ORBUMPS on the injection girder a laser beam can conceivably photoionize the H^- ions. A design of the laser interaction cavity is shown in Fig. 10. Experiments at LAMPF[2,4] have shown that the photodetachment of the loosely bound (.79 eV) outer electron is not difficult, however the inner electron will require a photon of considerably greater energy. The semirelativistic 200 MeV energy of the H^- particles can be used to effectively increase the energy of the photons involved in the Compton collisions; the relativistic Doppler shift is given by $\Delta = \gamma (1+\beta\cos \alpha) = 1.9$ at 200 MeV ($\alpha = 0$ when the H^- and γ are incident head on). Nonlinear crystals can be used to extract harmonics from the laser beam, quadrupling the photon energy but decreasing the beam intensity. The required photon energy is fixed by the desired orbital transition while the intensity and laser power are determined by the cross-section for the transition. High power Q-switched lasers are unacceptable because the photoionization must continue for the entire ~100 μsec injection period. H^- photodetachment and photoionization cross-sections have been theoretically calculated by Broad and Reinhardt[3]; their results appear in Figures 7,8,9.

LASER POWER CALCULATIONS

A = cross-sectional beam area

N_{BEAM} = number of H^- in a ~100 μsec beam squirt.

L_{INT} = length of interaction region between ORBUMPS

L_{BEAM} = length of a beam squirt.

N_H = number of H^- in the interaction region = $N_{BEAM} * \frac{L_{INT}}{L_{BEAM}}$

Probability of photoionization per atom = $p = \frac{\sigma N_H}{A}$.

To photoionize most H^- we require $N_\gamma = \frac{1}{p}$ per atom,

or $N_\gamma = \frac{N_H}{p} = \frac{A}{\sigma}$ = # photons in the interaction region.

The number of photons per ~100 μsec beam squirt = N_γ'.

$$N_\gamma' = N_\gamma \frac{L_{BEAM}}{L_{INT}} = \frac{A\ L_{BEAM}}{\sigma\ L_{INT}}.$$

Energy per beam squirt = $N_\gamma' * \hbar\omega = \frac{A\ L_{BEAM}}{\sigma\ L_{INT}} * \hbar\omega$.

If two mirrors are introduced (see Fig. 10) with a combined reflectivity of .99, then 200 photon transversals will occur before the intensity I drops to $\frac{I}{e}\ I_o$; 100 of these transversals will be in the proper direction to utilize the Doppler shift. The intensity is now increased by a conservative factor of 10 and the supplied energy E' can be decreased by the same factor.

$$\Rightarrow E' = \frac{A\ L_{BEAM} * \hbar\omega\ *\ 1.6\times10^{-19}\ J/eV}{\sigma\ L_{INT} *\ 10}$$

Power per beam squirt (instantaneous) = $\frac{E'}{T_{BEAM}}$

$$= \frac{A\hbar\omega\ *\ 1.6\times10^{-19}}{\sigma\ L_{INT} *\ 10}\ \frac{L_{BEAM}}{T_{BEAM}}$$

$$\text{Power} = \frac{A * \hbar\omega\ *\ 1.6\times10^{-19}}{\sigma\ *\ L_{INT} *\ 10}\ \beta c \text{ Watts.}$$

SINGLE PHOTON (BRUTE FORCE) PROCESS ($\hbar\omega + H^- \rightarrow H^+ + e^- + e^-$)

The maximum photoionization cross-section (Fig. 7) occurs at 17 eV which requires a laboratory frame photon in the UV, 1385 Å. Commercial lasers are not readily available in this range due to optical opacity. The lower limit of photon energy in the center of mass is ~14 eV, where $\sigma = 3\times10^{-20}$ cm^2. This implies a laser power of 10^9 watts (Assuming A = 2 cm^2) with 1680 Å lab frame photons; in 100 μsec the laser must deliver 100K Joules. Transmission through each of the two nonlinear crystals is probably not better than 50% and should the laser beam cross sectional size be greater than expected, the transmission goes as A^{-1}. This implies either a rather hefty laser of $\gtrsim 5\times10^9$ watts with ~6700 Å pre-quadrupling-crystal photons or near UV 3360 Å photons which need only be doubled. This lasing system is not feasible because of the exorbitant power-energy requirements, also the photon wavelength is quite far in the UV.

SELECTIVE TWO STEP (STS) PHOTOIONIZATION[5]

($\hbar\omega_1 + \hbar\omega_2 + H^- \rightarrow H^+ + e^- + e^-$)

The STS process requires two photons of different energy $\hbar\omega_1$ and $\hbar\omega_2$. The first photon detaches the outer electron and excites the inner electron to a higher energy state, while the second photon produces the final photoionization.

The power required to balance the downward transitions from the first excited state is $P_1 = \frac{\hbar\omega_1}{\sigma_1 T_1} \frac{\text{watts}}{\text{cm}^2}$, where

σ_1 = cross-section for transition from original to excited state.

T_1 = lifetime in excited state.

The photoionization probability of the excited state is given by $W_2 = \frac{\sigma_2 P_2}{\hbar\omega_2}$, where

σ_2 = cross-section for transition from excited state to continuum.

P_2 = intensity at frequency ω_2 (watts/cm^2), and

W_2 = probability/sec.

To photoionize most of the excited electrons, we require that the electron be hit by a photon before it executes a downward transition, i.e. $W_2 \gtrsim \frac{1}{T_1}$

$$\Rightarrow \frac{P_2}{P_1} = \frac{\hbar\omega_2 \; W_2 \; \sigma_1 \; T_1}{\sigma_2 \hbar\omega_1} \approx \frac{\omega_2 \sigma_1}{\omega_1 \sigma_2} \; .$$

If the intermediate state is the n = 2 orbital of H, then from Fig. 9 we find $\sigma_1 = 6.2\text{x}10^{-17}$ cm^2 at 10 eV. We can estimate σ_2 from Fig. 7, since σ_2 will be more probable than photoionizing from the ground state but much less probable than photodetaching the outer electron, $\Rightarrow \sigma_2 \approx 5\text{x}10^{-19} \rightarrow 10^{-18}$ at 10 eV. $T_1 \simeq 2\pi\text{x}10^{-8}$ sec,

$$\Rightarrow P_1 = \frac{\hbar\omega_1}{\sigma_1 T_1} = \frac{10\text{eV} * 1.6\text{x}10^{-19} \text{ J/eV}}{6.2\text{x}10^{-17} * 2\pi\text{x}10^{-8}} = 4\text{x}10^5 \text{ Watts}$$

$$P_2 \approx \frac{\sigma_1}{\sigma_2} P_2 = 2.5\text{x}10^7 \text{ Watts}$$

If mirrors are used, both P_1 and P_2 can be decreased by a factor of 10. The resulting powers of $P_1 = 10^5$W and $P_2 = 5\text{x}10^6$W (on 2 cm^2) are much lower than the single photon process power of $\sim 5\text{x}10^9$ Watts. Moreover, the lab frame photons (5.2 eV, 2350 Å) require a 4700 Å laser with one doubling crystal which is in a much more feasible part of the spectrum. A tunable laser for the first exci-

tation is essential to coincide with the narrow absorption line.

III JETS

Liquid and gas jets are currently being successfully used as accelerator targets and should be adaptable to stripping applications. H_2 jets at STP are unworkable since they would have to be ~2cm thick (80% stripping) and would expand into the booster vacuum, and the scattering would be tremendous. Mercury jets need to be ~.05 μ thick (90% conversion), a range which is accessible to the jet system.

IV CONCLUSIONS

Several systems seem to promise an elegant and trouble-free solution to the stripping problem. Lithium and Beryllium foils should be made and irradiated to determine durability and scattering. It seems unlikely that even the strongest of the high Z metals can retain tensile strength and the required thicknesses. Electroplating of Be and Li in a manner analogous to parylene foils might be easier than rolling and would undoubtedly produce a more regular surface which seems to significantly affect scattering. Lasers are theoretically elegant but seem to be technically difficult, and should probably be pursued only after exhausting mercury and other jets for which the specific technology has already been developed. These high power lasers will most likely be rather large, and the available tunnel space must be considered.

The following people were very helpful in preparing this paper: Chuck Ankenbrandt, Howard Bryant, Cy Curtis, Chuck Schmidt, Jim Griffin, Rolland Johnson, and Lee Teng.

REFERENCES

1) G. J. Marmer, "Stripping Efficiency for the process $H^- \rightarrow H^0$", Argonne National Laboratory Technical Note, 2/12/69.

2) H.C. Bryant and P.A. Lovoi, "Production of pulsed particle beams by photodetachment of H^-", Phys. Rev. letters 27(24), 12/13/71.

3) J.T. Broad and W.P. Reinhardt, "One-and Two-electron photoejection from H^-: a multi-channel J-matrix calculation", available from W.P. Reinhardt, Joint Institute for laboratory astrophysics, University of Colorado, Boulder, Colorado 80309. To be published in Phys. Rev., 1976-1977.

4) LAMPF proposal #200,"A study of the photodetachment spectrum of H^- in the vicinity of 11 eV", Los Alamos Scientific Lab, Los Alamos, N.M.

5) R.V. Ambartzumian and V.S. Letokhov, Selective Two-Step (STS) photoionization of atoms and photodissociation of Molecules by Laser radiation", Applied Optics, Vol II No. 2, February 1972.

Fig. 1. Conversion Efficiency vs. R.M.S Scattering Angle

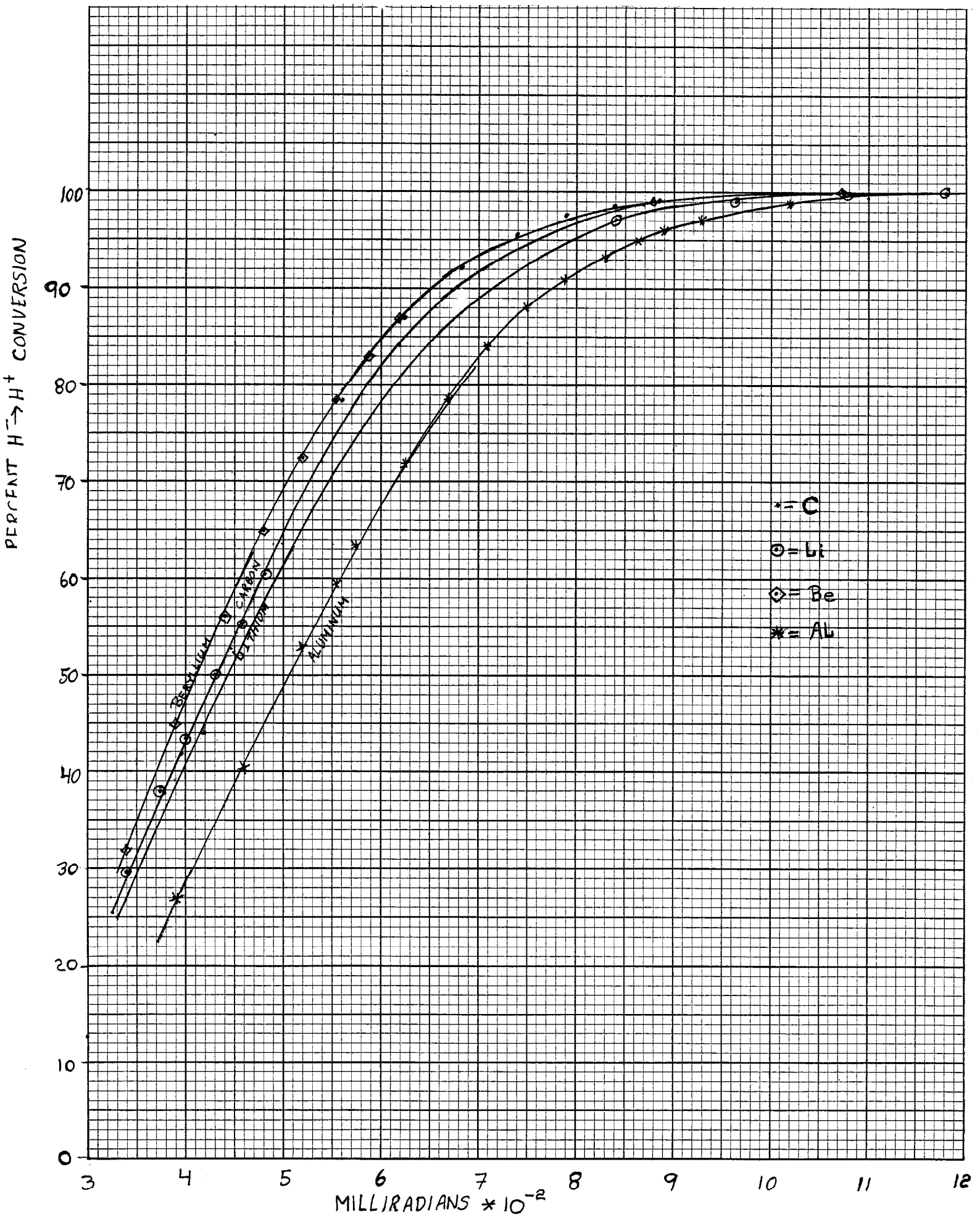

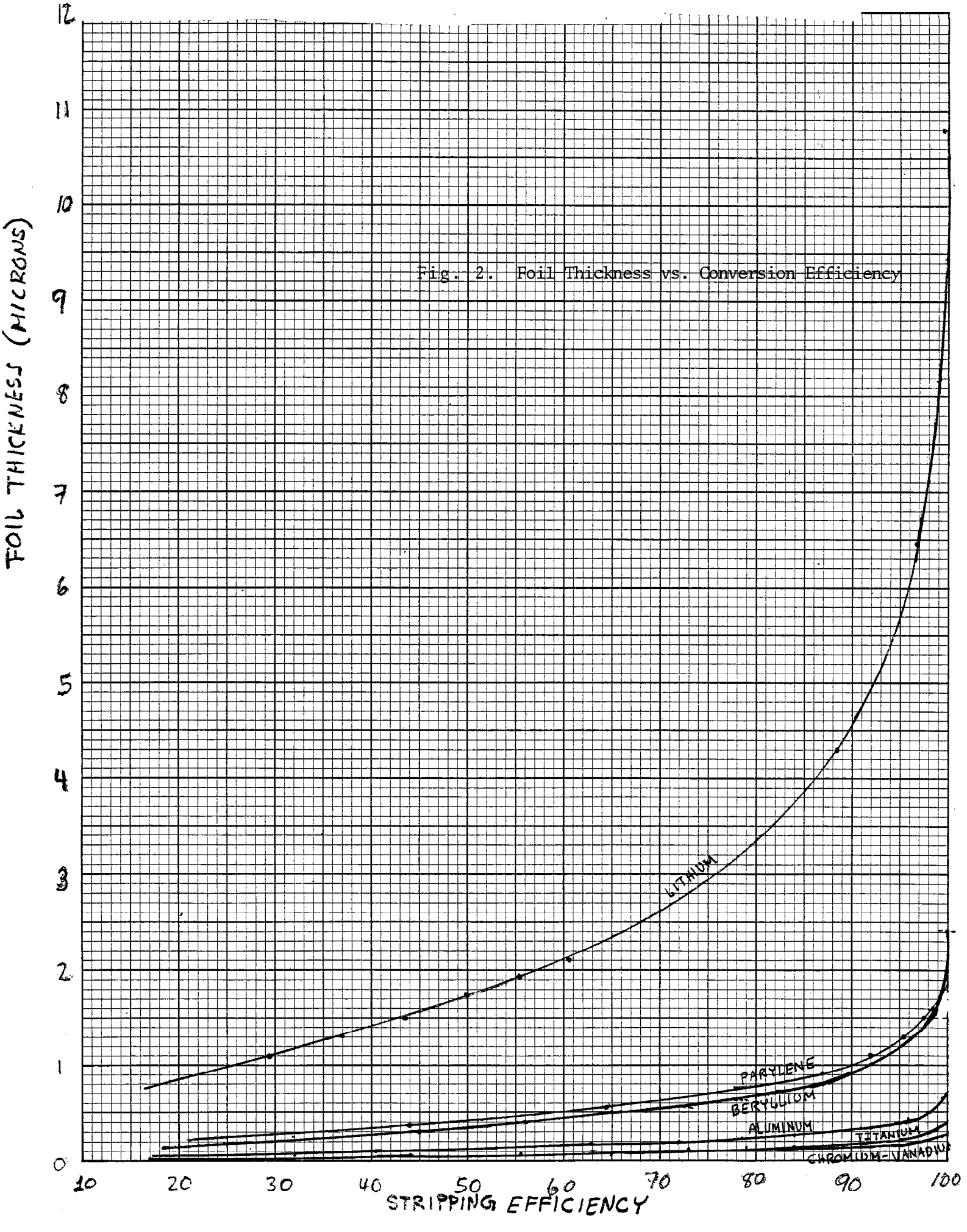

Fig. 2. Foil Thickness vs. Conversion Efficiency

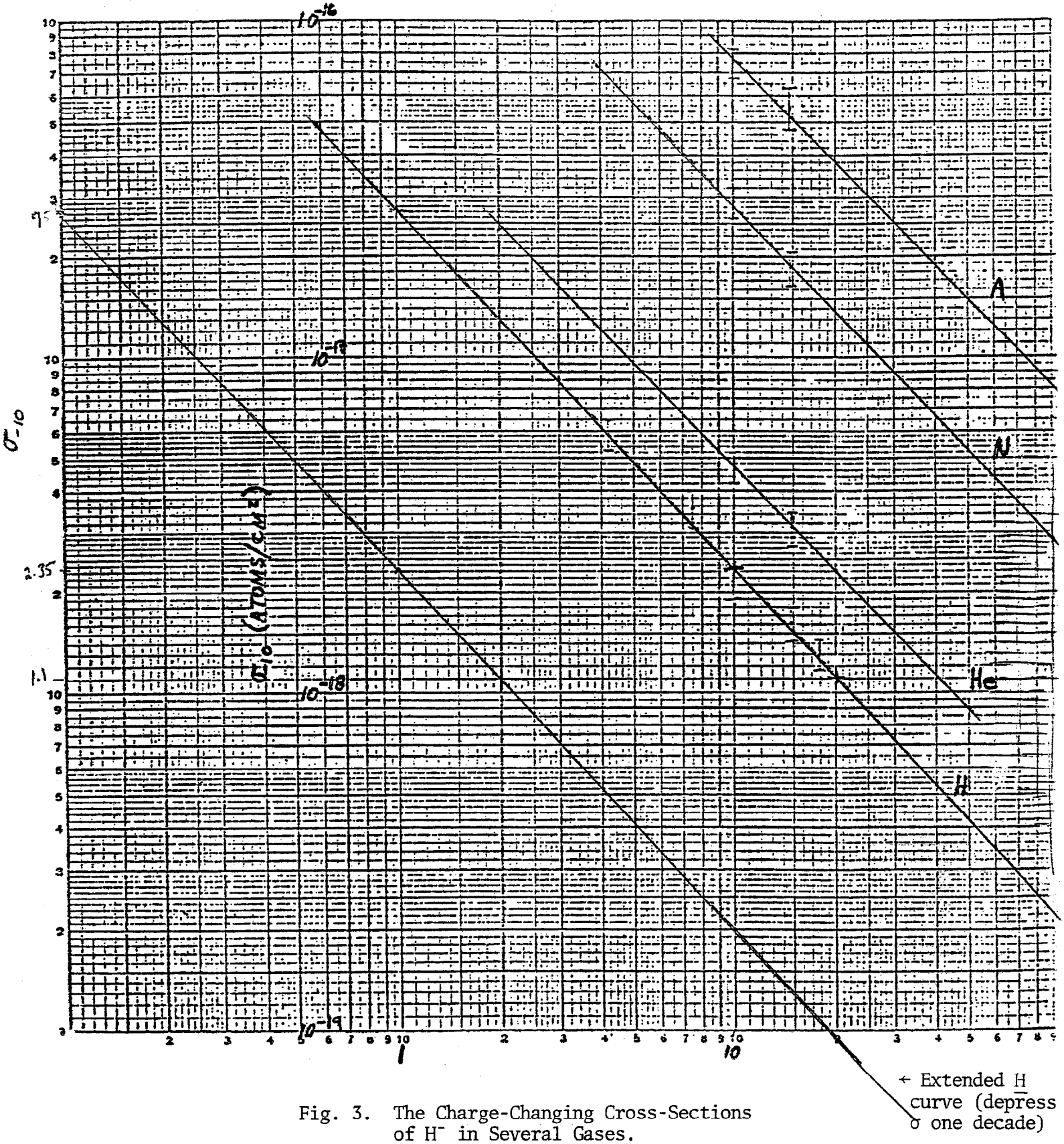

Fig. 3. The Charge-Changing Cross-Sections of H^- in Several Gases.

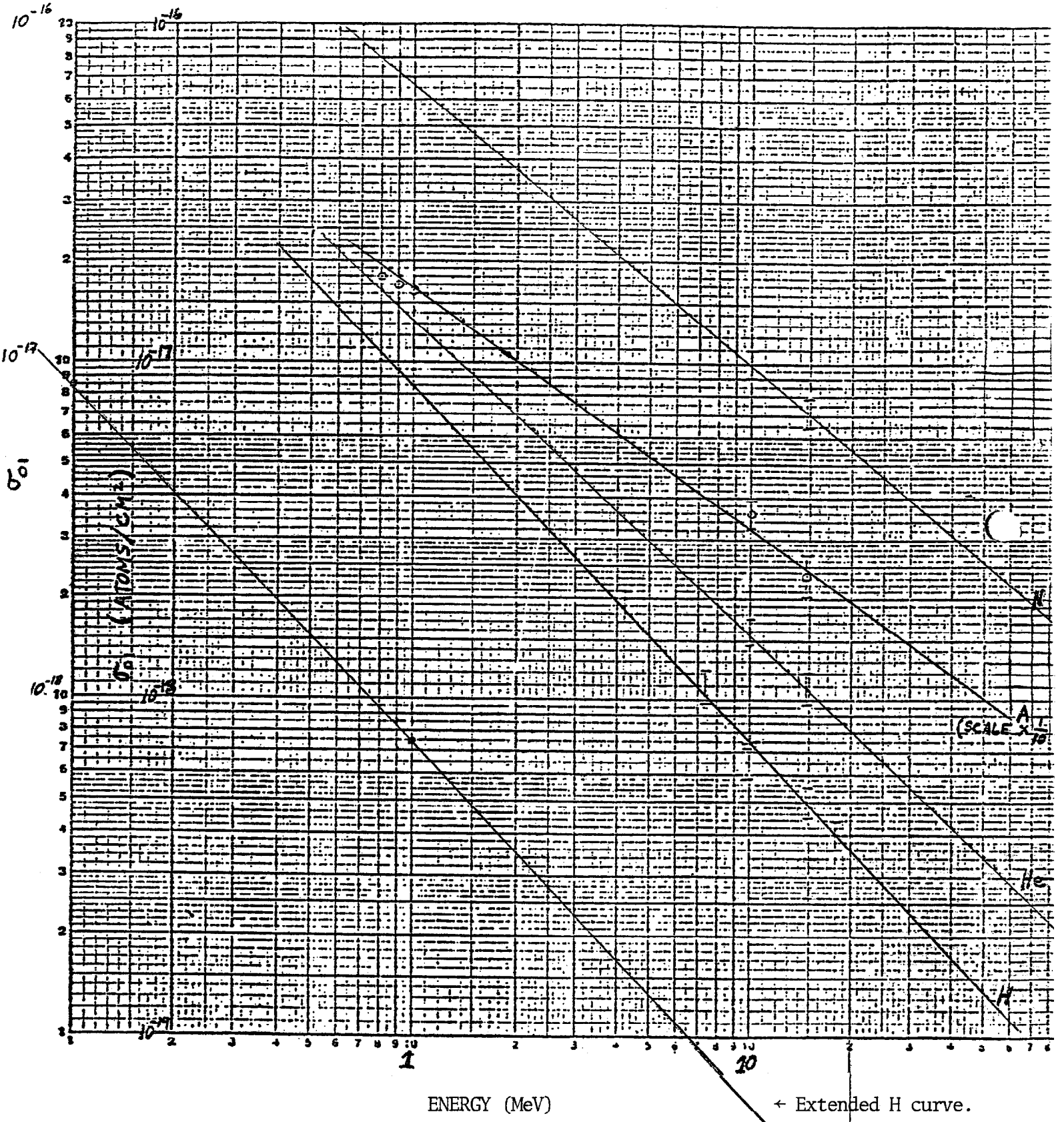

Fig. 3a: The Charge-Changing Cross-Sections of H^0 in Several Gases. Note that the Cross-Sections in Argon are depressed by one decade for ease in drawing.

Fig. 4. Cross-Section σ vs. Z at 200 MeV

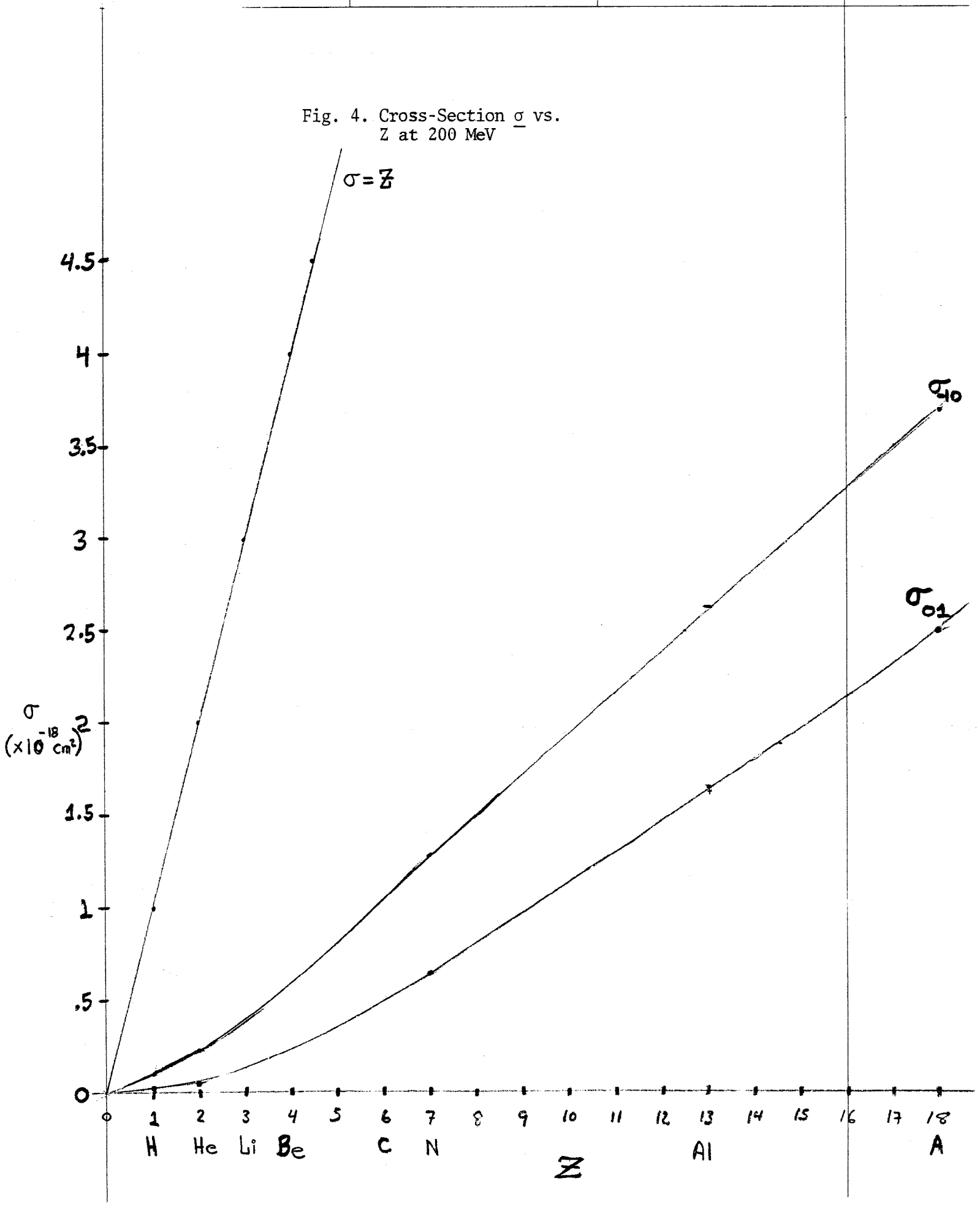

E in MeV	Boron (I = 57.5 ev)		Carbon (I = 69 ev)	
	Energy Loss $(-\frac{dE}{dx})$	Range	Energy Loss $(-\frac{dE}{dx})$	Range
0		0		0
1	2.42467×10^{-1}	2.890	2.41758×10^{-1}	2.760
2	1.44542	8.4550	1.49676	8.1130
3	1.05529	1.66485×10	1.09761	1.59838×10
4	8.40700×10^{-2}	2.73305	8.75831×10^{-2}	2.62925
5	7.03397	4.04064	7.33961	3.88859
6	6.07363	5.57560	6.34518	5.35789
7	5.36113	7.33162	5.60616	7.03867
8	4.80635	9.30499	5.03354	8.92378
9	4.36942	1.14905×10^{2}	4.57573	1.10106×10^{2}
10	4.00899	1.38826	4.20066	1.32935
11	3.70811×10^{-2}	1.64782	3.88732	
12	3.45285	1.92749	3.62130	1.84374
13	3.23335	2.22697	3.39243	
14	3.04245	2.54597	3.19326	2.43321
15	2.87479	2.88425	3.01826	
16	2.72627	3.24160	2.86317	3.09577
17	2.59374	3.61779	2.72471	
18	2.47468	4.01262	2.60039	3.82973
19	2.36710	4.42591	2.48783	
20	2.26939	4.85748	2.38565	4.63358
25	1.88953		1.98812	
30	1.62761	1.01441×10^{3}	1.71372	9.65798
35	1.43545		1.51222	
40	1.28811×10^{-2}	1.71063×10^{3}	1.35762×10^{-2}	1.62667×10^{3}
45	1.17135		1.23504	
50	1.07642	2.56400	1.13533	2.43603
55	9.97656×10^{-3}		1.05256	
60	9.31220	3.50604	9.82726×10^{-3}	3.38580
65	8.74326		9.22900 -	
70	8.25089	4.70951	8.71124	4.46908
75	7.82082		8.25809	
80	7.44035	5.98793	7.85829	5.67979
85	7.10259		7.50276	
90	6.80024	7.39565	7.18446	7.01242
95	6.52797		6.89777	
100	6.28146	8.92731	6.63817	8.46197
125	5.33120		5.63703	
150	4.68484	1.82853×10^{4}	4.95568	1.73119×10^{4}
175	4.21641		4.46169	
200	3.86146	3.01278	4.08726	2.85450
225	3.58311		3.79356	
250	3.35934	4.40695	3.55741	4.16715
275	3.17563		3.35463	
300	3.02229	5.98040	3.20164	5.65534

Fig. 5. Ranges of Protons in Boron and Carbon (in Mg/cm^2) and Energy Losses (in $MeV/mg/cm^2$).

(Note milligram units)

Fig. 6. Foil Specifications

COMPOSITION	Z	A	$\rho(g/cm^3)$	σ_{-10} (cm^2)	σ_{01} (cm^2)	L_{RAD} (g/cm^2)	
Lithium	3	7	.534	3.75×10^{-19}	1.25×10^{-19}	83.3	$\varepsilon = .2$
Beryllium	4	9.1	1.848	6×10^{-19}	2.5×10^{-19}	66	$\varepsilon = .35$
Parylene	6	12	1.1	1×10^{-18}	5×10^{-19}	43.3	
Aluminum	13	27	2.7	2.6×10^{-18}	1.6×10^{-18}	24.3	
Titanium	22	48	4.54	$\sim 4.5 \times 10^{-18}$	$\sim 3.25 \times 10^{-18}$		
Vanadium	23	51	6.11	$\sim 4.7 \times 10^{-18}$	$\sim 3.4 \times 10^{-18}$		
Chromium	24	52	7.2	$\sim 4.9 \times 10^{-18}$	$\sim 3.6 \times 10^{-18}$		
Mercury	80	200.6	~13.5	$\sim 2.1 \times 10^{-17}$	$\sim 1.7 \times 10^{-17}$		

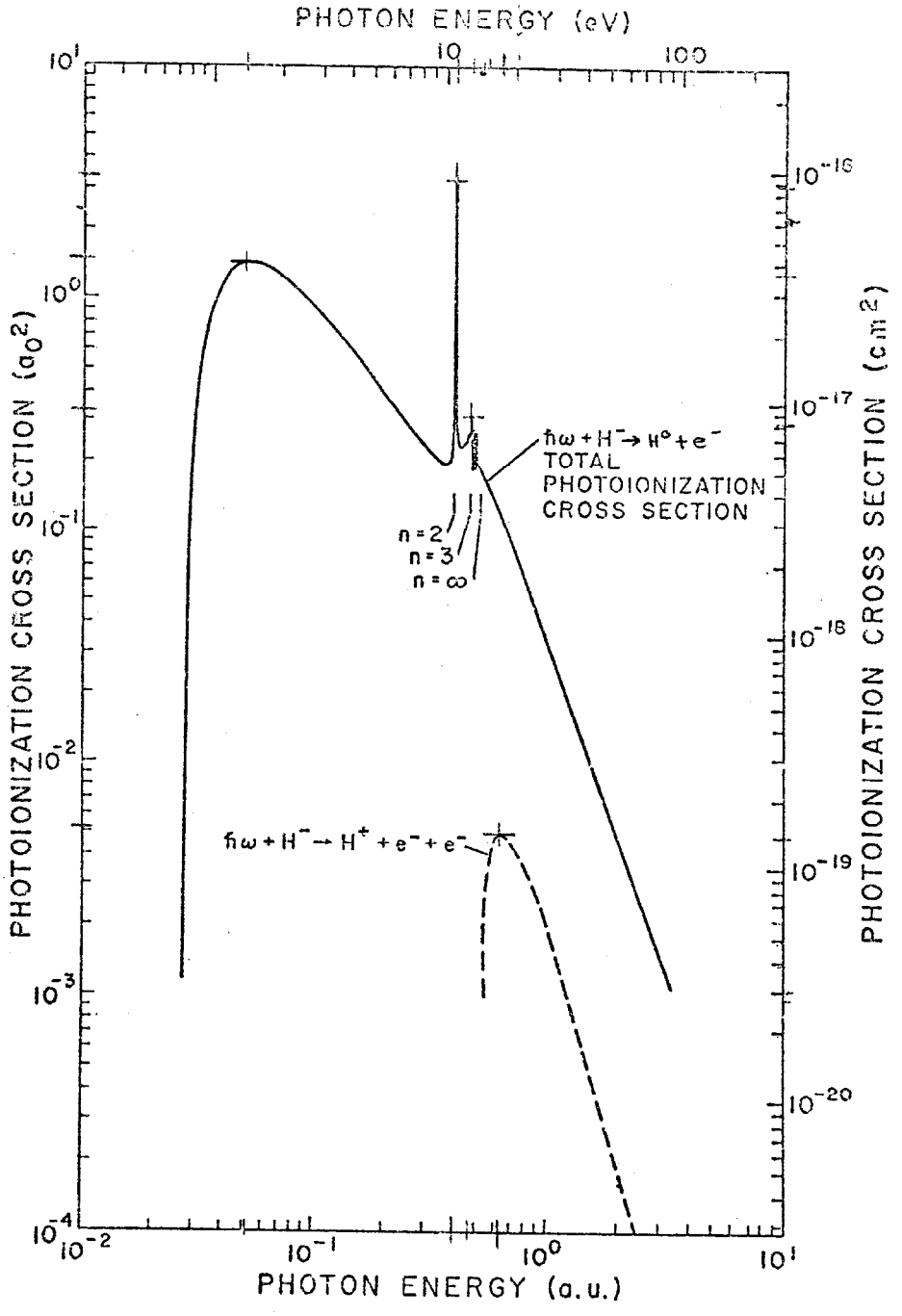

Fig. 7. H^- photodetachment cross-section and two electron ejection cross-section. The two electron ejection cross-section is smoothed version of Fig. 8.

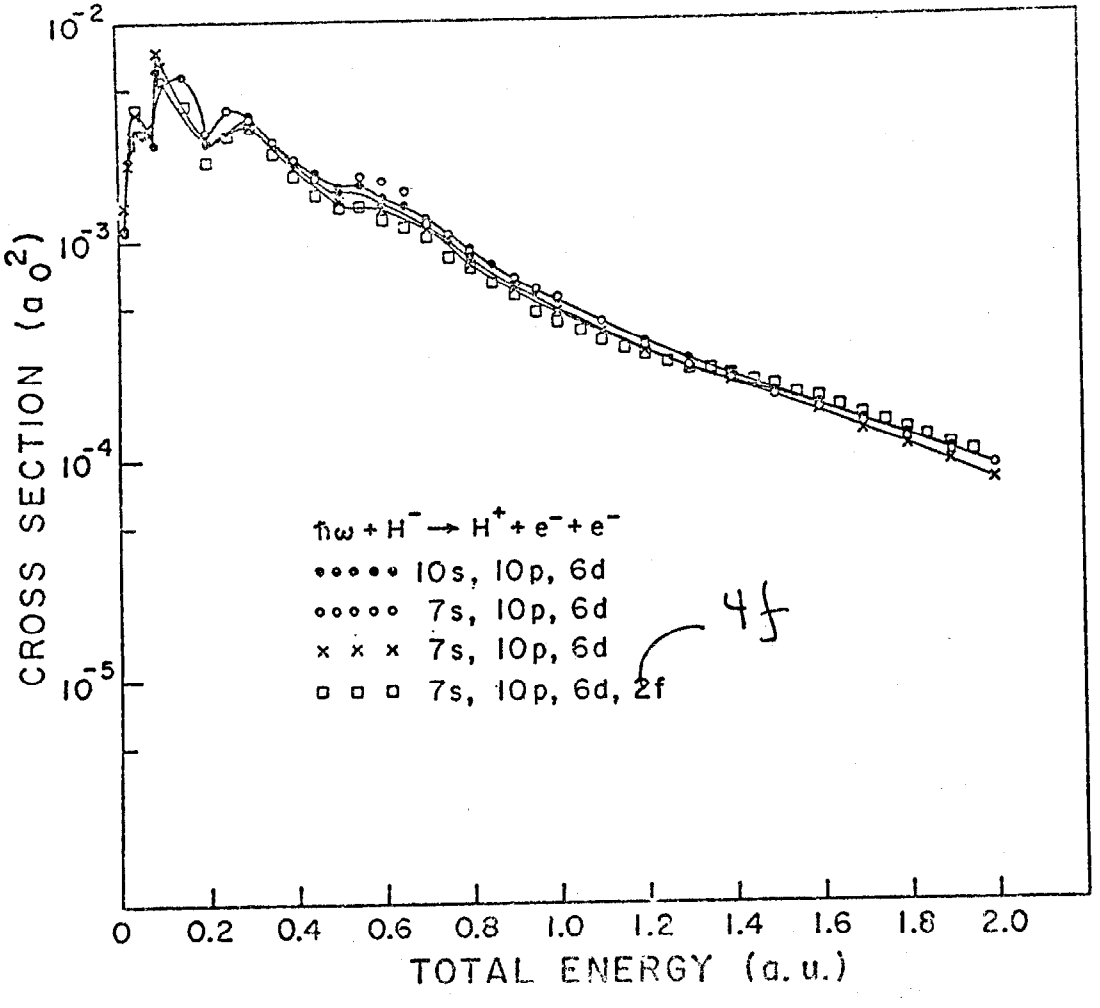

Fig. 8. Cross-section for two Electron Photoejection.

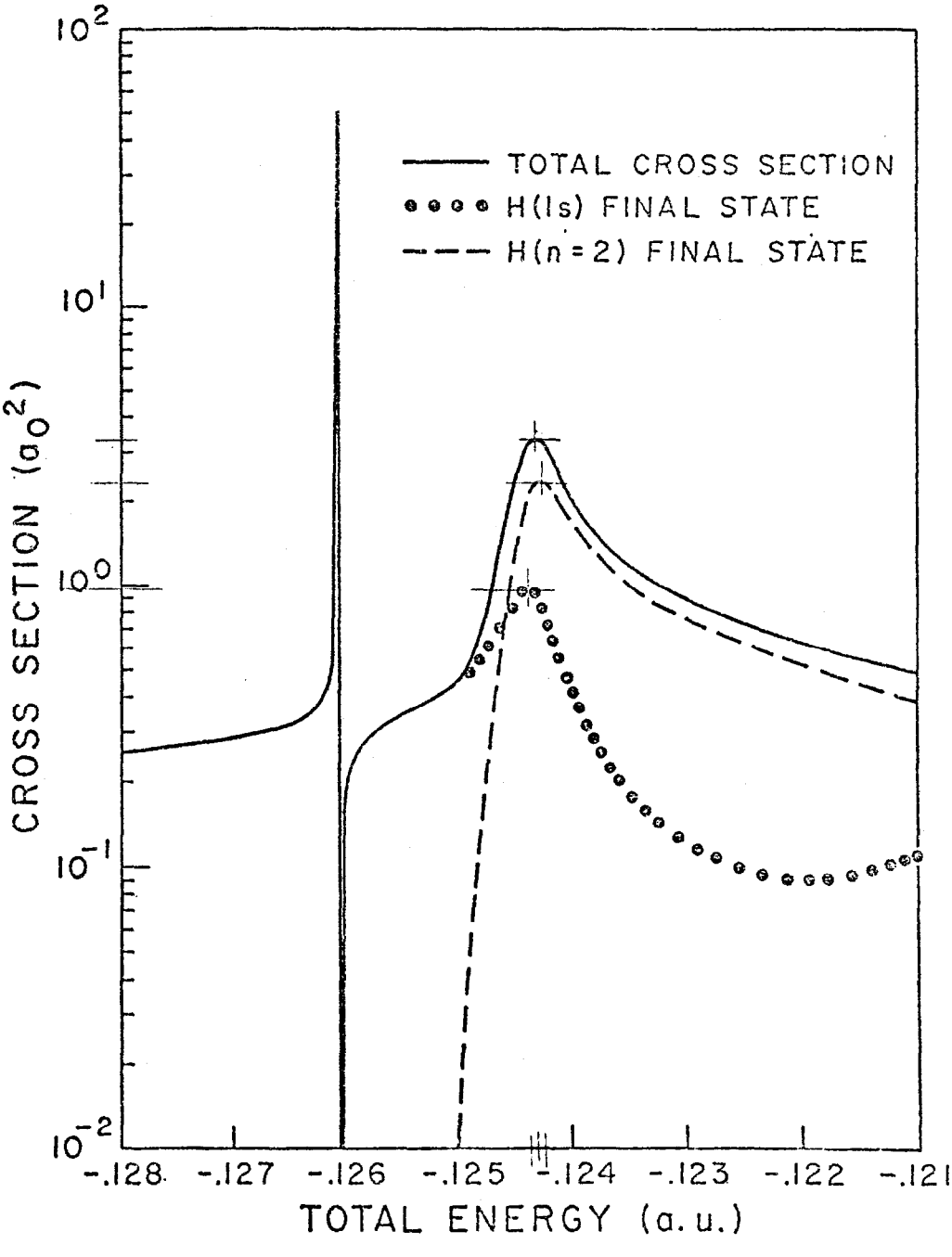

Fig. 9. H^- Photodetechment Resonance Structure near the n = 2 Threshold.

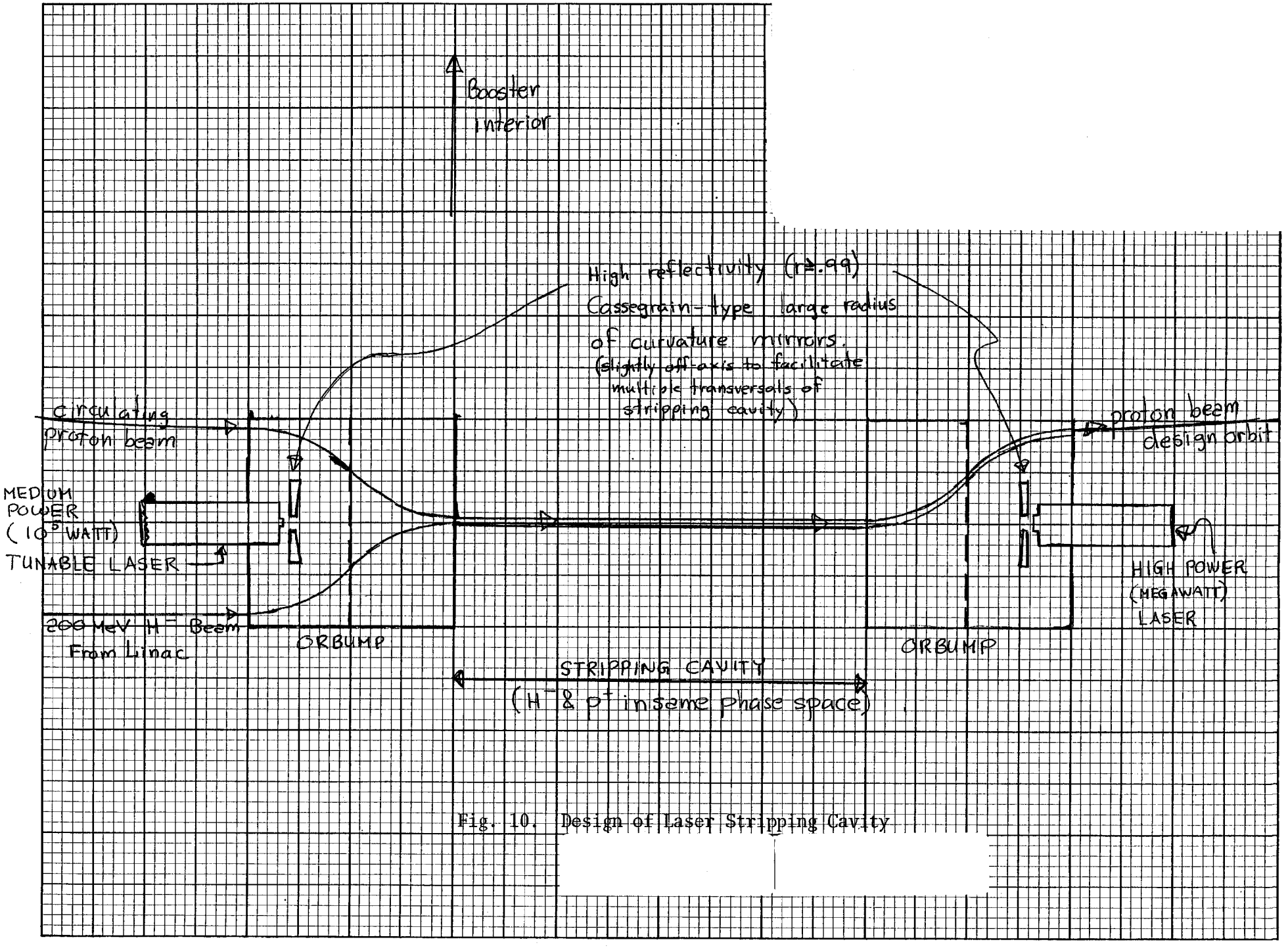

Fig. 10. Design of Laser Stripping Cavity